Facile synthesis of the nitrogen-rich covalent organic framework for efficient capture of iodine

Nowsheenah Farooq, Abu Taha, Athar Adil Hashmi*

Department of Chemistry, Jamia Millia Islamia, New-Delhi-110025, India

Corresponding author Email: ahashmi@jmi.ac.in

Tel.: +91 8800705490

Chemicals and Materials

4-hydroxy benzaldehyde and cyanuric chloride were purchased from Sigma-Aldrich. Iodine and potassium iodide were obtained from Merck. All additional chemicals, including solvents and reagents used in this research were sourced locally. Triazine trialdehyde was synthesized according to a previously published article [1].

Synthesis of monomer triazine core trialdehyde (TTT):

Triazine core trialdehyde was synthesized according to a previously published article [1]. 4-Hydroxybenzaldehyde weighing 7.4 g (61 millimoles), and sodium hydroxide, weighing 2.5 grams (62 millimoles), were dissolved in 100 milliliters of mixture of acetone and water (1:1 v/v). The resulting solution was gradually added, one drop at a time into a stirred solution containing cyanuric chloride weighing 3.7 grams (20 millimoles), dissolved in 50 ml of acetone, while maintaining a temperature of 0 °C for a duration of 1 hour. The reaction mixture was subjected to reflux for a duration of two hours and subsequently, it was poured into 300 mL of water, resulting in the formation of a white solid product. The obtained product was washed with water and 10 % Na_2CO_3, then vacuum dried to yield white powder. This white powder was further purified by recrystallization using ethyl acetate to yield a white crystalline solid.

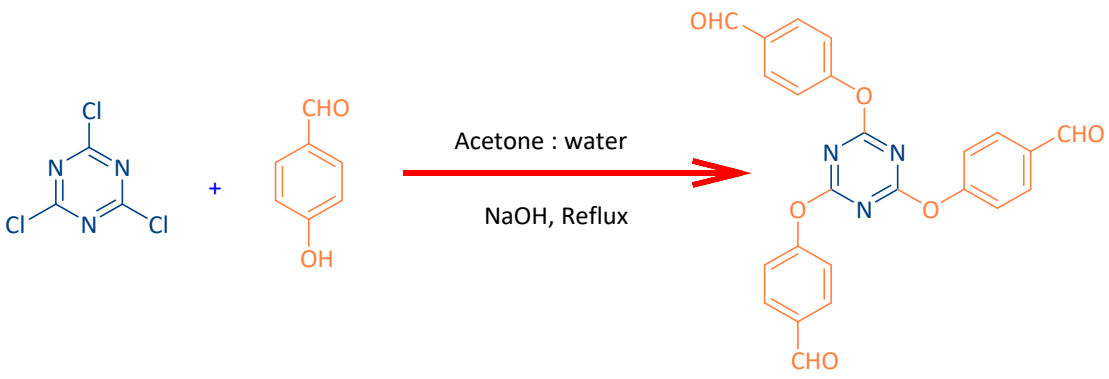

TTT

Synthesis of NR_COF-C1

Triazine trialdehyde (**TTT**) (1 mmol, 0.44g), benzene-1,4-diamine **(BD)** (1.45 mmol, 0.156 g), and THF (10 ml) in a round-bottom flask equipped with a condenser and stir bar. An aqueous acetic acid as a catalyst (6 M, 0.5 ml) was added to the resultant heterogeneous mixture after 10 minutes of stirring and heated at 65 °C. The reaction was carried out for 72 hours under an inert atmosphere and the wine brownish product obtained was cooled at room temperature, filtered, washed with methanol and acetone, and dried under vacuum at 80 °C as a brown powder (yield 0.288 g), and was used for analyses.

Table S1: Solubility/insolubility chart of NR_COF-C1.

Organic solvents	**Solubility**
Dimethyl Sulfoxide	Insoluble
Dimethylformamide	Insoluble
Dimethylacetamide	Insoluble
Methanol	Insoluble
Acetonitrile	Insoluble
Dichloromethane	Insoluble
Ethyle acetate	Insoluble
Hexane	Insoluble
chloroform	Insoluble
Tetrahydrofuran	Insoluble

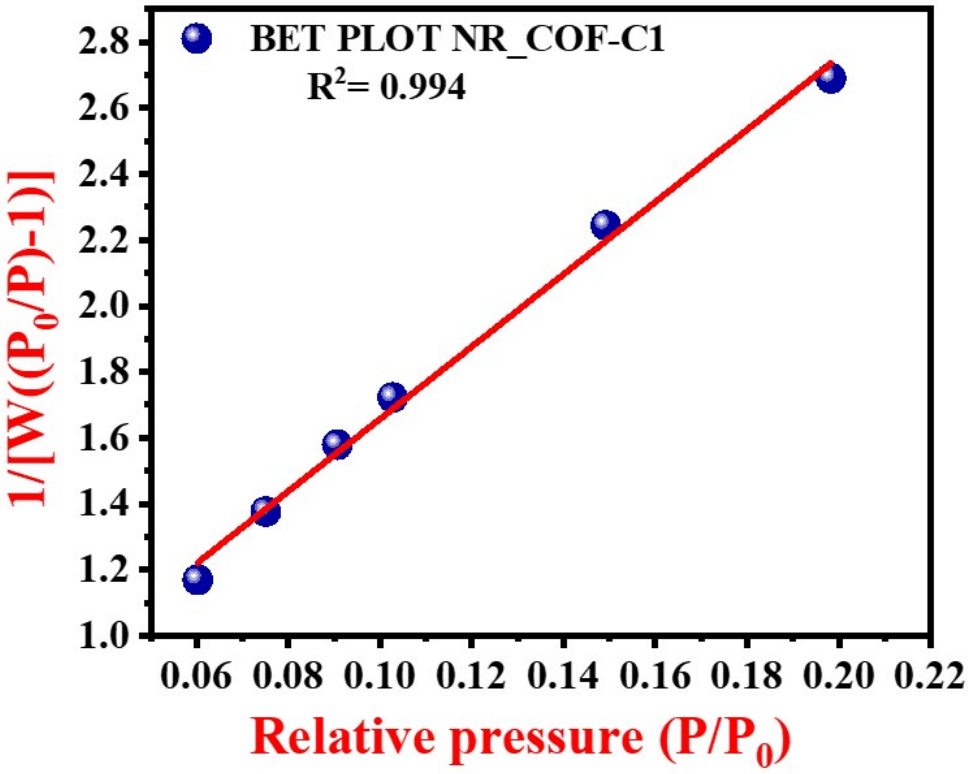

Fig. S1: BET plot of NR_COF-C1

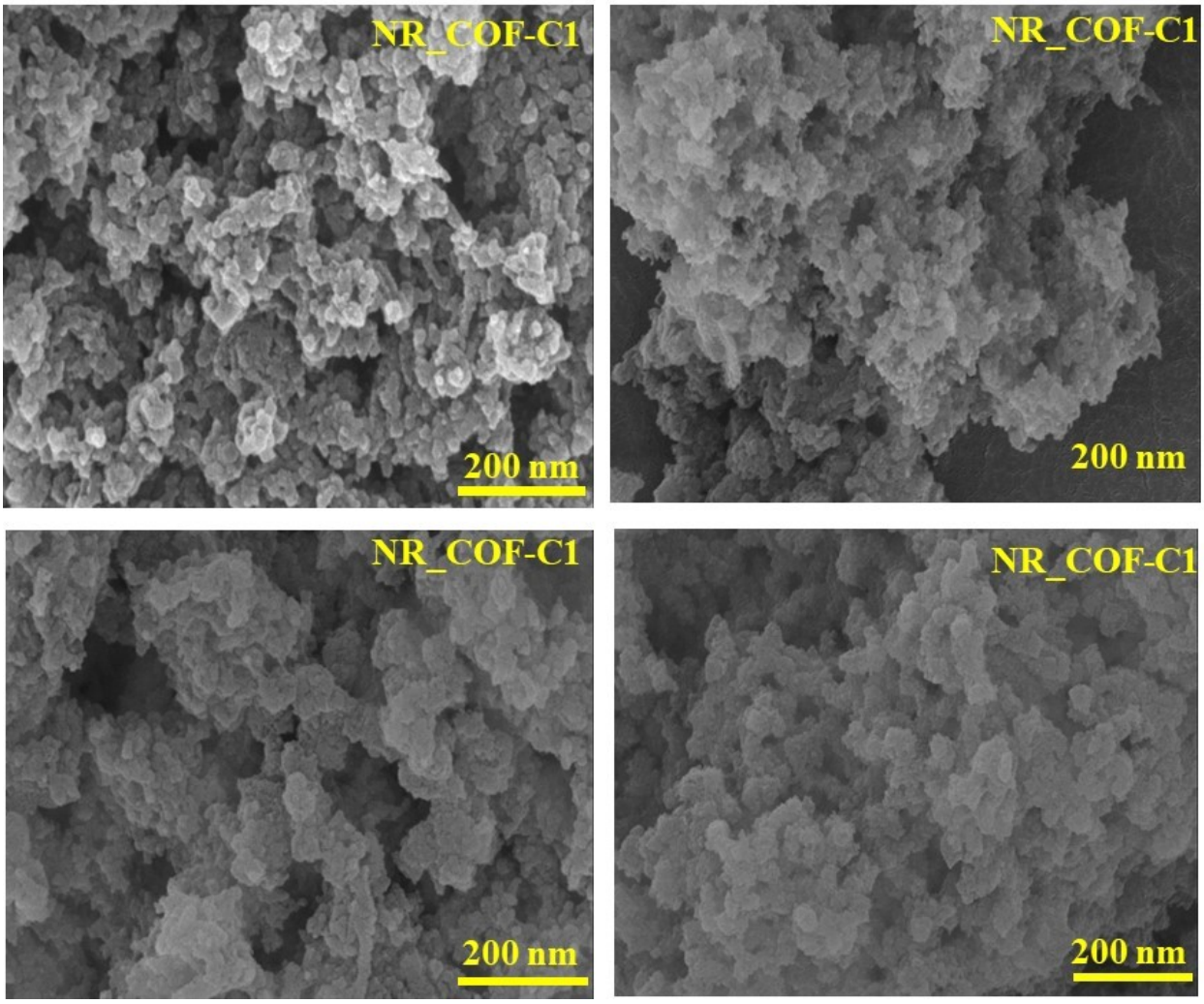

Fig S2. FE-SEM images of NR_COF-C1

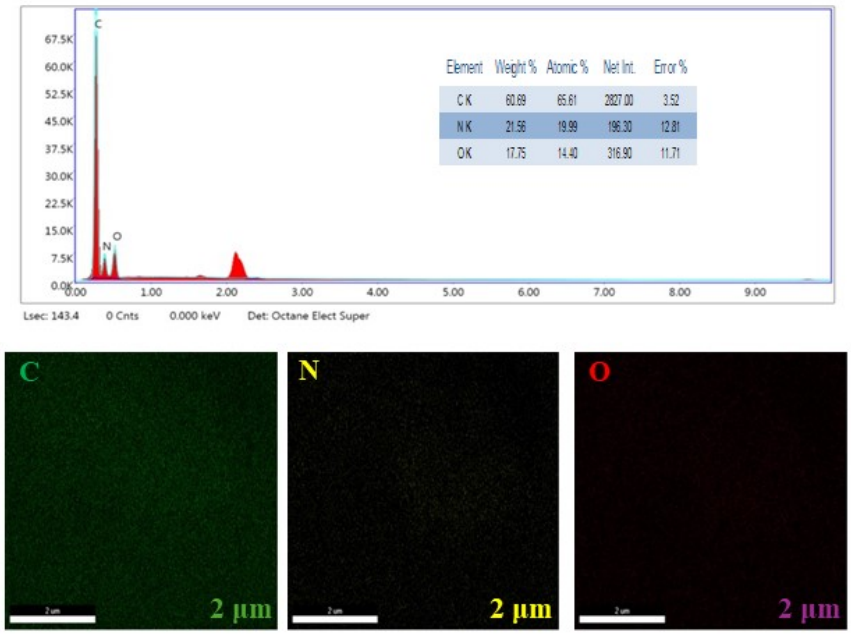

Fig. S3: EDX analysis of NR_COF-C1

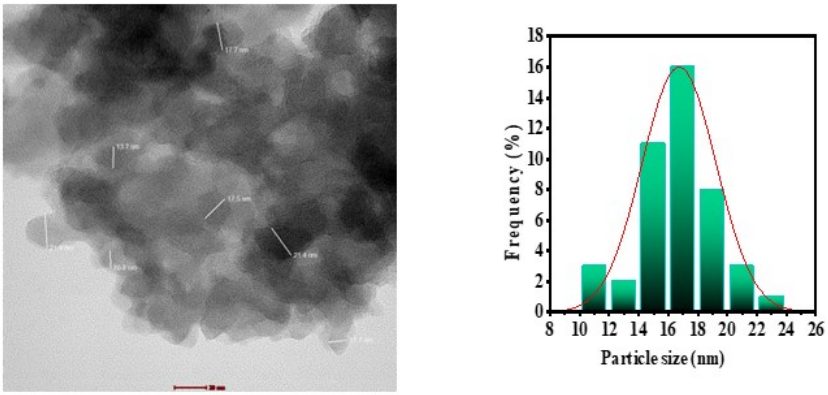

Fig. S4: TEM image of NR_COF-C1 with average particle size graph

Iodine sorption experiments

In vapor phase

20 mg of NR_COF-C1 was precisely weighed and deposited in a 5 ml glass vial. This 5 ml vial was then placed inside a 15 ml glass vial and finally this setup was placed in a larger 50 ml glass chamber containing iodine granules. The glass chamber was sealed and subjected to heating at 75 °C and 1.0 bar pressure. At specified time intervals, the 15 ml vial containing NR_COF-C1 sample was taken out, cooled, cleaned carefully, and weighed. The observed increase in mass was noted before placing it back. The iodine adsorption capacity of NR_COF-C1 was calculated using equation 1.

$$\alpha = \frac{M_2 - M_1}{M_1} \qquad \text{eq 1.}$$

Where α is the weight percent of iodine captured, M_2 and M_1 are the masses of samples after and before iodine adsorption.

The data was fitted with non-linear equation for pseudo-second order kinetic model.

$$Q_t = \frac{K_2 Q_e^2 t}{1 + K_2 Q_e t} \qquad \text{eq 2.}$$

Here, Qe and Qt represent the quantity of iodine uptake (g/g) at equilibrium and the quantity of iodine adsorbed (g/g) at any given time t respectively. k2 (g/g/hour) is the pseudo-second-order rate constant.

Kinetic experiment

To collect the data on the rate of iodine uptake capacity from aqueous solution, an experiment was conducted by taking 2.5 mg of NR_COF-C1 and added to 5 ml of 50 ppm I_3^- solution. At different time intervals, the supernatants were taken, and their UV-vis spectra was recorded. The percentage of iodine captured was determined using the formula:

$$\%\, removal = \frac{C_0 - C_t}{C_0} * 100\ \% \qquad \text{eq 3.}$$

where C_0 and C_t are the initial concentration in water at the start of the experiment and at time t, respectively. The data was fitted with non-linear equation for pseudo-second order kinetic model.

$$Q_t = \frac{K_2 Q_e^2 t}{1 + K_2 Q_e t} \qquad \text{eq 2.}$$

Here, Q_t and Q_e refer to the adsorbed amount of iodine (mg/g) at any time (t) and at equilibrium respectively. K_2 (g/mg/min) are that rate constants of the above mentioned pseudo-second-order equation.

Uptake capacity determination

50 mg weight of NR_COF-C1 was measured and added in an aqueous solution containing KI_3 (600 mg KI and 300 mg I_2 in 3 ml of water) for a period of 48 hours. After this specific time interval, the adsorbent was isolated through filtration and washed with water till filtrate achieved clarity. The iodine uptake capacity of NR_COF-C1 was found to be 4850.75 mg/g.

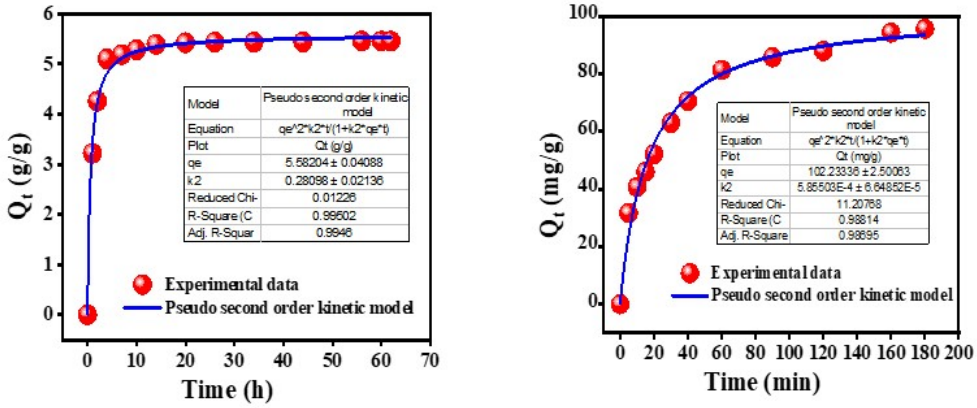

Fig. S5: (a) Pseudo second order kinetic model applied to adsorbtion of iodine vapors by NR_COF-C1 (b) Pseudo second order kinetic model applied to adsorption of iodine by NR_COF-C1 from aqueous solution

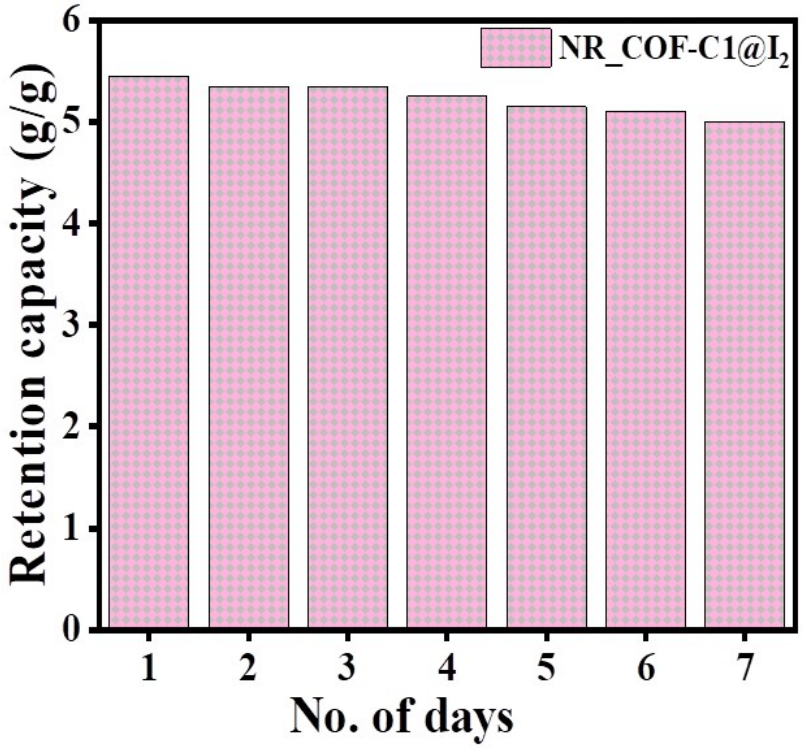

Fig. S6: Data of iodine retention experiment of NR_COF-C1@I_2

This experiment in aqueous phase was repeated multiple times as shown:

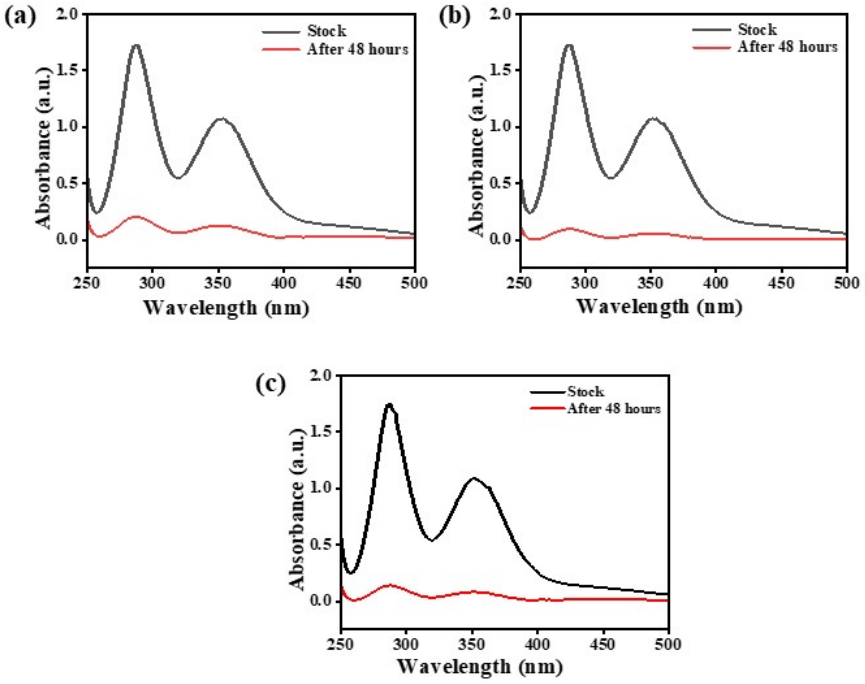

Fig. S7: UV-vis graphs of repeated experiments of iodine adsorption by NR-COF-C1 from aqeous phase

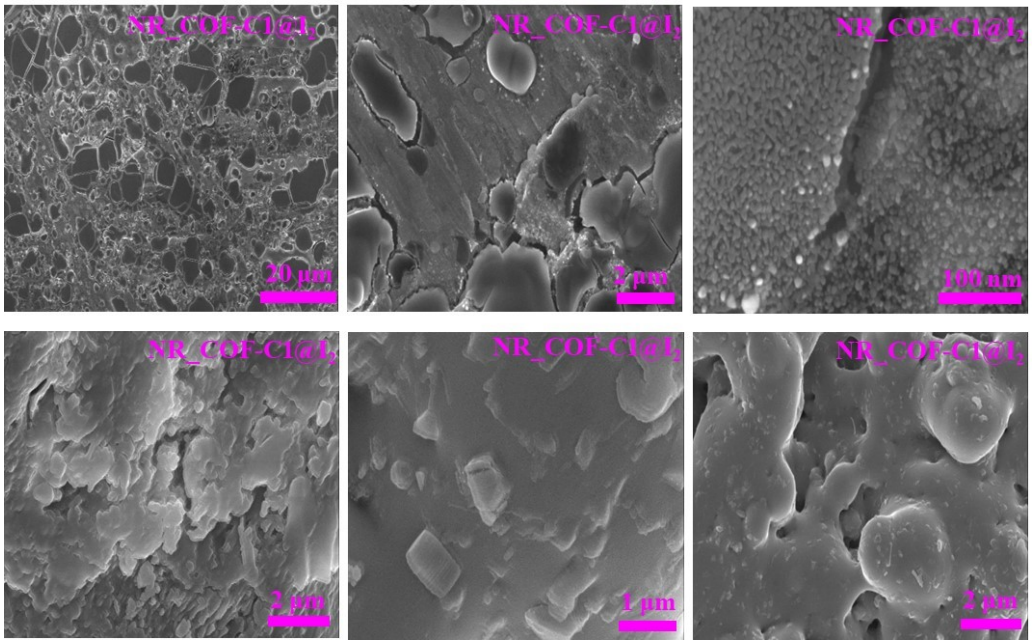

Fig. S8: FE-SEM images of NR_COF-C1@I_2

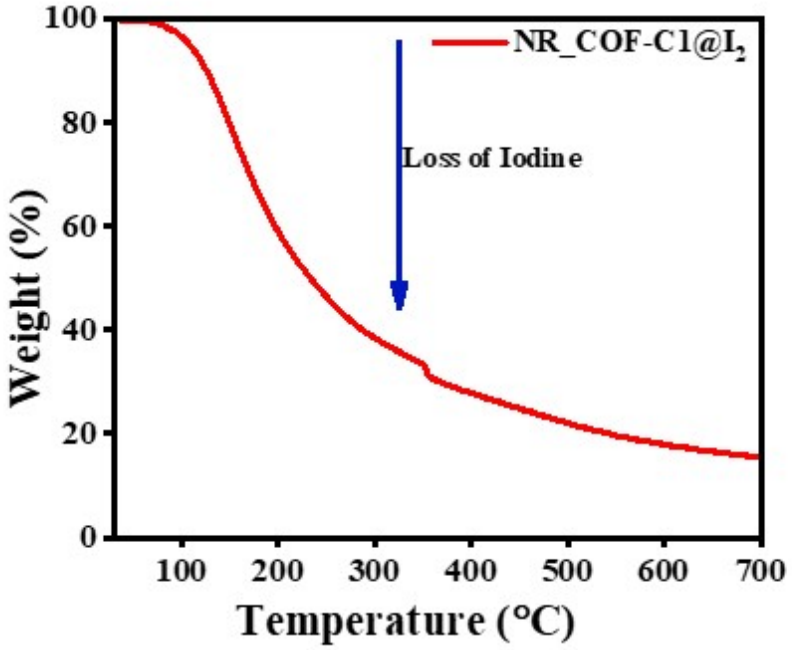

Fig. S9: TGA analysis of NR_COF-C1@I_2

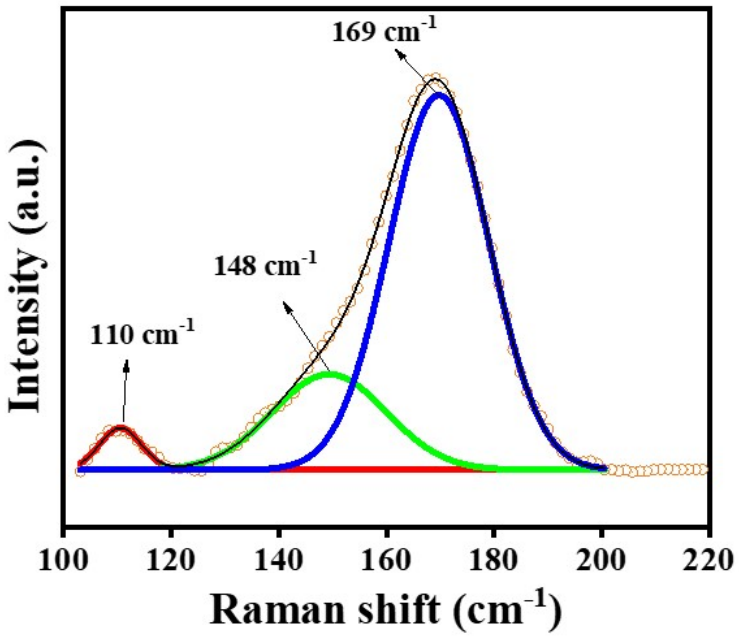

Fig. S10: Raman spectra of NR_COF-C1 before and after iodine capture

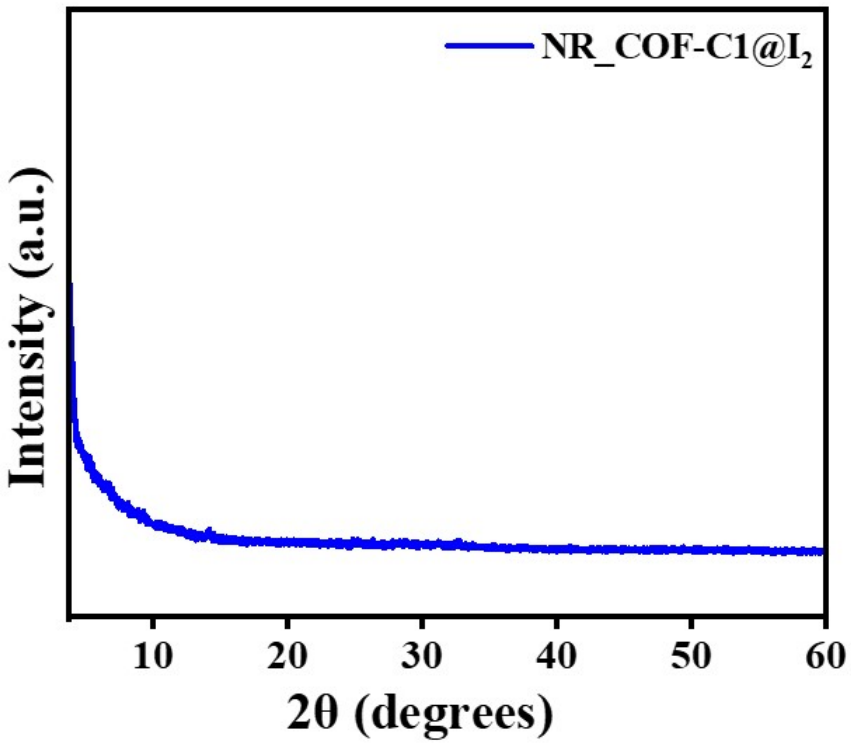

Fig. S11: PXRD plot of NR_COF-C1@I_2

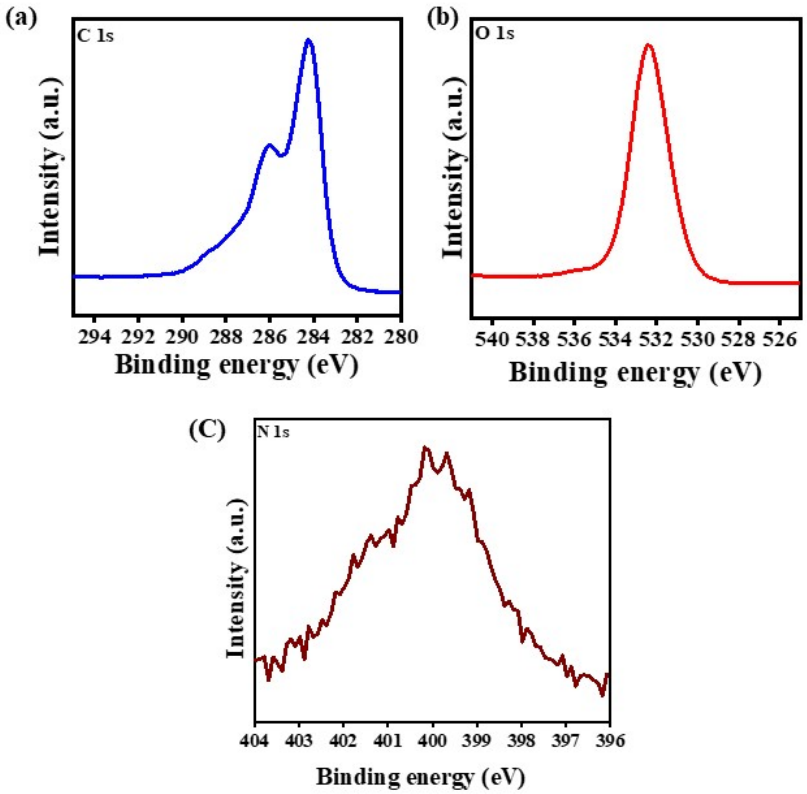

Fig. S12: XPS spectra of (a) C 1s (b) O 1s and (c) N 1s of NR_COF-C1

Iodine release and regeneration of adsorbent NR_COF-C1 on heating:

To study the iodine desorption 20 mg of this NR_COF-C1@I_2 was taken in an open glass vial and heated at 125 °C for 300 minutes in oven under ambient pressure. At specific time intervals of the experiment the change in mass of sample was noted and its iodine release efficiency (Re) was calculated by the equation below:

$$Re = \frac{20 - Mt}{Mx} * 100\ wt\% \qquad \text{eq 4.}$$

Where Mt is the weight of polymer after time t (t ranges from 0-400 min) and Mx is the weight of iodine adsorbed in 20 mg of NR_COF-C1@I_2.

Iodine release and NR_COF-C1 regeneration in methanol:

For the desorption of iodine in methanol,15 mg of iodized covalent organic polymer NR_COF-C1@I_2 was loaded in glass vial screw-on cap and 5 ml of methanol was added. With the elapse of time, the color change of solution from yellow to dark brown was observed due to release of iodine from NR_COF-C1@I_2 into the methanol. The experiment was carried out for 35 hours and UV-visible spectrophotometry was recorded at regular intervals for the gradual iodine release in methanol. The two absorbance peaks appeared in the UV-vis spectra with two maxima at 290 nm and 360 nm while using methanol as solvent.

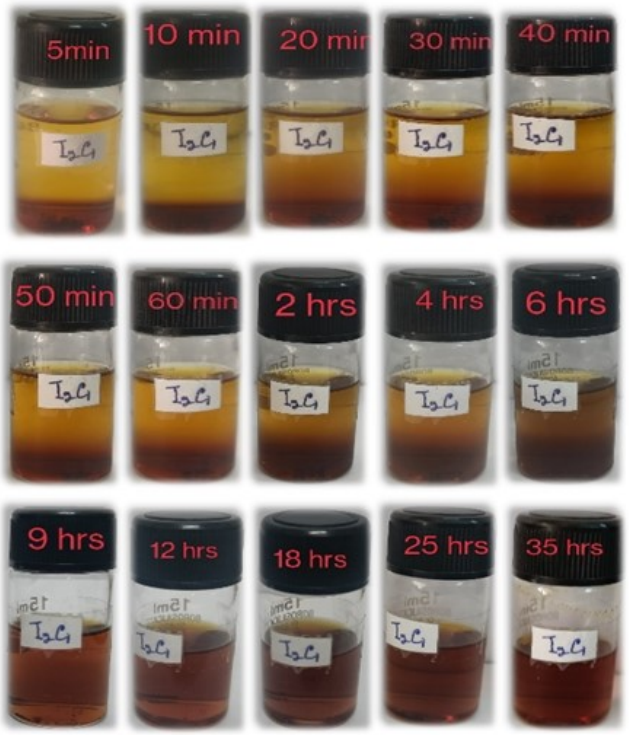

Fig. S13: Digital images of gradual iodine release in methanol from NR_COF-C1@I_2

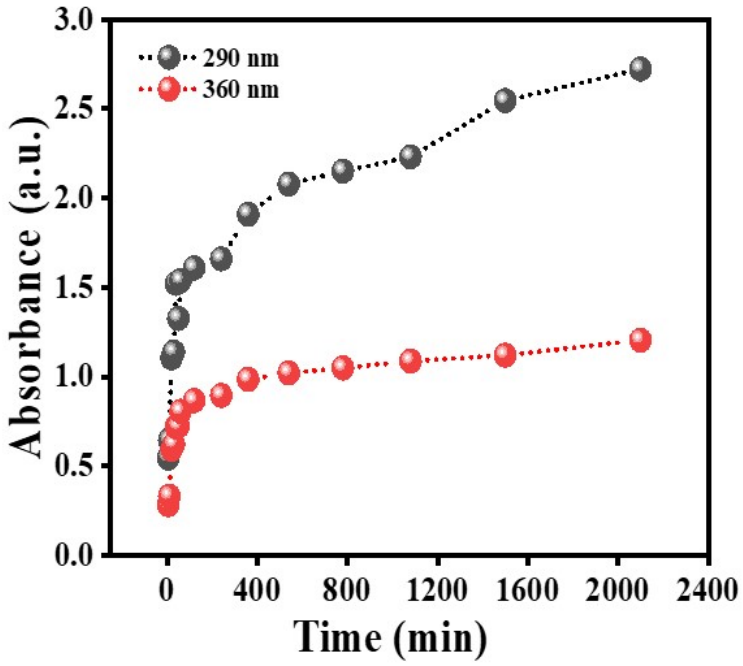

Fig. S14: Monitoring release of iodine release from NR_COF-C1@I_2

Table S2: Comparison Table of Iodine vapor capture by adsorbents at high temperatures

Adsorbents	**Temperature (°C)**	**BET Surface area (m^2/g)**	**I_2 uptake (g/g)**	**References**
TPB-DMTP COF	75	1927	6.260	[2]
TJNU-201	77	2510	5.625	[3]
NR_COF-C1	**75**	**175**	**5.45**	**This work**
NDB-H	75	117	4.430	[4]
CMP-LS4	77	462	3.32	[5]
PHF-1-Ct PHF-1	80	690 1046	4.05 3.05	[6]
HCMP-3	75	92	3.36	[7]
POP-1	80	12	3.570	[8]
Micro-COF-1 Micro-COF-2	75	816 1056	2.9 3.5	[9]
Azo-Trip	77	510.4	2.36	[10]
PAN-B PAN-T	75	1254 1273	3.17 3.11	[11]
N-HCP	75	6.44	2.57	[12]
CMPN-3	70	1368	2.080	[13]
ZIF-8	77	1630	1.25	[14]
AlOC-26-NC AlOC-27-NC	80	508 285	0.70 0.50	[15]

Table S3: Comparison table of iodine adsorption by adsorbents at room temperature (R.T.)

Adsorbents	**Temperature (°C)**	**BET Surface area(m^2/g)**	**I_2 uptake (g/g)**	**References**
iCOF-AB-50	R.T.	1390	2.790	[16]
NR_COF-C1	**R.T.**	**175**	**2.15**	**This work**
SCU-COF-2	R.T.	413.4	0.98	[17]
AC	R.T.	NR	0.70	[18]
HISL	R.T.	NR	0.53	[18]
SL-1	R.T.	NR	0.48	[18]
CC3	20	NR	0.36	[19]
ZIF-8	R.T.	NR	0.03	[18]

NR=Not reported

Table S4: Comparison table of iodine adsorption by adsorbents from aqueous solution

Adsorbents	**Medium**	**BET Surface area (m^2/g)**	**I_2 uptake (mg/g)**	**References**
NR_COF-C1	**Water**	**175**	**4850.75**	**This work**
HcOF-1	Water	NR	2900	[20]
TP_POP-7	Water	86	2312	[21]
PCN-223-HPP	Water	851.271	1676.960	[22]
Fe_3O_4@PPy	Water	NR	1627	[23]
PCN-223	Water	642.089	1615.882	[22]
TAPB-BPDA COF	Water	1082	988.17	[24]
MBM - MOF	Water	62	880	[25]

References

[1] X. Guo, Y. Tian, M. Zhang, Y. Li, R. Wen, X. Li, X. Li, Y. Xue, L. Ma, C. Xia, S. Li, Mechanistic Insight into Hydrogen-Bond-Controlled Crystallinity and Adsorption Property of Covalent Organic Frameworks from Flexible Building Blocks, Chem. Mater. 30 (2018) 2299–2308. https://doi.org/10.1021/acs.chemmater.7b05121.

[2] P. Wang, Q. Xu, Z. Li, W. Jiang, Q. Jiang, D. Jiang, Exceptional Iodine Capture in 2D Covalent Organic Frameworks, Adv. Mater. 30 (2018). https://doi.org/10.1002/adma.201801991.

[3] J. Li, H. Zhang, L. Zhang, K. Wang, Z. Wang, G. Liu, Y. Zhao, Y. Zeng, Two-dimensional covalent–organic frameworks for ultrahigh iodine capture, J. Mater. Chem. A. 8 (2020) 9523–9527. https://doi.org/10.1039/C9TA13980J.

[4] Z. Guo, P. Sun, X. Zhang, J. Lin, T. Shi, S. Liu, A. Sun, Z. Li, Amorphous Porous Organic Polymers Based on Schiff-Base Chemistry for Highly Efficient Iodine Capture, Chem. – An Asian J. 13 (2018) 2046–2053. https://doi.org/10.1002/asia.201800698.

[5] C. Feng, G. Xu, W. Xie, S. Zhang, C. Yao, Y. Xu, Polytriazine porous networks for effective iodine capture, Polym. Chem. 11 (2020) 2786–2790. https://doi.org/10.1039/C9PY01948K.

[6] K. Jie, H. Chen, P. Zhang, W. Guo, M. Li, Z. Yang, S. Dai, A benzoquinone-derived porous hydrophenazine framework for efficient and reversible iodine capture, Chem. Commun. 54 (2018) 12706–12709. https://doi.org/10.1039/C8CC07529H.

[7] Y. Liao, J. Weber, B.M. Mills, Z. Ren, C.F.J. Faul, Highly Efficient and Reversible Iodine Capture in Hexaphenylbenzene-Based Conjugated Microporous Polymers, Macromolecules. 49 (2016) 6322–6333. https://doi.org/10.1021/acs.macromol.6b00901.

[8] X. Qian, B. Wang, Z.-Q. Zhu, H.-X. Sun, F. Ren, P. Mu, C. Ma, W.-D. Liang, A. Li, Novel N-rich porous organic polymers with extremely high uptake for capture and reversible storage of volatile iodine, J. Hazard. Mater. 338 (2017) 224–232. https://doi.org/10.1016/j.jhazmat.2017.05.041.

[9] S. An, X. Zhu, Y. He, L. Yang, H. Wang, S. Jin, J. Hu, H. Liu, Porosity Modulation in Two-Dimensional Covalent Organic Frameworks Leads to Enhanced Iodine Adsorption

Performance, Ind. Eng. Chem. Res. 58 (2019) 10495–10502. https://doi.org/10.1021/acs.iecr.9b00028.

[10] Q.-Q. Dang, X.-M. Wang, Y.-F. Zhan, X.-M. Zhang, An azo-linked porous triptycene network as an absorbent for CO 2 and iodine uptake, Polym. Chem. 7 (2016) 643–647. https://doi.org/10.1039/C5PY01671A.

[11] C. Liu, M. Xia, M. Zhang, K. Yuan, F. Hu, G. Yu, X. Jian, One-pot synthesis of nitrogen-rich aminal- and triazine-based hierarchical porous organic polymers with highly efficient iodine adsorption, Polymer (Guildf). 194 (2020) 122401. https://doi.org/10.1016/j.polymer.2020.122401.

[12] X. Li, Y. Peng, Q. Jia, Construction of hypercrosslinked polymers with dual nitrogen-enriched building blocks for efficient iodine capture, Sep. Purif. Technol. 236 (2020) 116260. https://doi.org/10.1016/j.seppur.2019.116260.

[13] Y. Chen, H. Sun, R. Yang, T. Wang, C. Pei, Z. Xiang, Z. Zhu, W. Liang, A. Li, W. Deng, Synthesis of conjugated microporous polymer nanotubes with large surface areas as absorbents for iodine and CO 2 uptake, J. Mater. Chem. A. 3 (2015) 87–91. https://doi.org/10.1039/C4TA04235B.

[14] D.F. Sava, M.A. Rodriguez, K.W. Chapman, P.J. Chupas, J.A. Greathouse, P.S. Crozier, T.M. Nenoff, Capture of Volatile Iodine, a Gaseous Fission Product, by Zeolitic Imidazolate Framework-8, J. Am. Chem. Soc. 133 (2011) 12398–12401. https://doi.org/10.1021/ja204757x.

[15] S. Yao, W.-H. Fang, Y. Sun, S.-T. Wang, J. Zhang, Mesoporous Assembly of Aluminum Molecular Rings for Iodine Capture, J. Am. Chem. Soc. 143 (2021) 2325–2330. https://doi.org/10.1021/jacs.0c11778.

[16] Y. Xie, T. Pan, Q. Lei, C. Chen, X. Dong, Y. Yuan, J. Shen, Y. Cai, C. Zhou, I. Pinnau, Y. Han, Ionic Functionalization of Multivariate Covalent Organic Frameworks to Achieve an Exceptionally High Iodine-Capture Capacity, Angew. Chemie. 133 (2021) 22606–22614. https://doi.org/10.1002/ange.202108522.

[17] L. He, L. Chen, X. Dong, S. Zhang, M. Zhang, X. Dai, X. Liu, P. Lin, K. Li, C. Chen, T.

Pan, F. Ma, J. Chen, M. Yuan, Y. Zhang, L. Chen, R. Zhou, Y. Han, Z. Chai, S. Wang, A nitrogen-rich covalent organic framework for simultaneous dynamic capture of iodine and methyl iodide, Chem. 7 (2021) 699–714. https://doi.org/10.1016/j.chempr.2020.11.024.

[18] T.C.T. Pham, S. Docao, I.C. Hwang, M.K. Song, D.Y. Choi, D. Moon, P. Oleynikov, K.B. Yoon, Capture of iodine and organic iodides using silica zeolites and the semiconductor behaviour of iodine in a silica zeolite, Energy Environ. Sci. 9 (2016) 1050–1062. https://doi.org/10.1039/C5EE02843D.

[19] T. Hasell, M. Schmidtmann, A.I. Cooper, Molecular Doping of Porous Organic Cages, J. Am. Chem. Soc. 133 (2011) 14920–14923. https://doi.org/10.1021/ja205969q.

[20] Y. Lin, X. Jiang, S.T. Kim, S.B. Alahakoon, X. Hou, Z. Zhang, C.M. Thompson, R.A. Smaldone, C. Ke, An Elastic Hydrogen-Bonded Cross-Linked Organic Framework for Effective Iodine Capture in Water, J. Am. Chem. Soc. 139 (2017) 7172–7175. https://doi.org/10.1021/jacs.7b03204.

[21] A. Hassan, A. Alam, S. Chandra, Prince, N. Das, Triptycene-based and imine linked porous uniform microspheres for efficient and reversible scavenging of iodine from various media: a systematic study, Environ. Sci. Adv. 1 (2022) 320–330. https://doi.org/10.1039/D2VA00024E.

[22] R. Liu, W. Zhang, Y. Chen, C. Xu, G. Hu, Z. Han, Highly efficient adsorption of iodine under ultrahigh pressure from aqueous solution, Sep. Purif. Technol. 233 (2020) 115999. https://doi.org/10.1016/j.seppur.2019.115999.

[23] D.K.L. Harijan, V. Chandra, T. Yoon, K.S. Kim, Radioactive iodine capture and storage from water using magnetite nanoparticles encapsulated in polypyrrole, J. Hazard. Mater. 344 (2018) 576–584. https://doi.org/10.1016/j.jhazmat.2017.10.065.

[24] R. Chen, T. Hu, Y. Li, Stable nitrogen-containing covalent organic framework as porous adsorbent for effective iodine capture from water, React. Funct. Polym. 159 (2021) 104806. https://doi.org/10.1016/j.reactfunctpolym.2020.104806.

[25] T. He, X. Xu, B. Ni, H. Lin, C. Li, W. Hu, X. Wang, Metal–Organic Framework Based Microcapsules, Angew. Chemie Int. Ed. 57 (2018) 10148–10152.

https://doi.org/10.1002/anie.201804792.